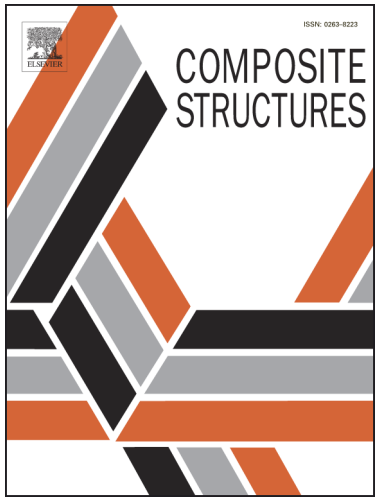

Fully reversible reinforcement of softwood beams with unbonded composite plates

Marco Corradi, Antonio Borri, Giulio Castori, Emanuela Speranzini

PII: S0263-8223(16)30253-7
DOI: http://dx.doi.org/10.1016/j.compstruct.2016.04.014
Reference: COST 7378

To appear in: *Composite Structures*

Received Date: 18 February 2016
Revised Date: 30 March 2016
Accepted Date: 6 April 2016

Please cite this article as: Corradi, M., Borri, A., Castori, G., Speranzini, E., Fully reversible reinforcement of softwood beams with unbonded composite plates, *Composite Structures* (2016), doi: http://dx.doi.org/10.1016/j.compstruct.2016.04.014

Fully reversible reinforcement of softwood beams with unbonded composite plates

Marco CORRADI

Corresponding author,

Mechanical and Construction Engineering Department, Northumbria University Wynne-Jones Building, NE1 8ST, Newcastle upon Tyne, United Kingdom and Department of Engineering, University of Perugia, Via Duranti, 93 06125 Perugia, Italy

email marco.corradi@northumbria.ac.uk

Tel. +44 (0) 191 243 7649, Fax. +44 (0) 191 227 4561

Antonio BORRI

Department of Engineering, University of Perugia

Via Duranti, 93 06125 Perugia, Italy

Giulio CASTORI

Department of Engineering, University of Perugia

Via Duranti, 93 06125 Perugia, Italy

Emanuela SPERANZINI

Department of Engineering, University of Perugia

Via Duranti, 93 06125 Perugia, Italy

ABSTRACT

In this paper, results of flexure tests aimed at improving the structural behaviour of softwood beams reinforced with unglued composite plates and at developing an effective alternative to the use of organic resins are presented. The addition of modest ratios of GFRP (*Glass Fiber Reinforced Polymer*) composite strengthening can prevent tension failure in timber beams. However the application of organic matrices presents problems of reversibility, compatibility and durability with timber and poor performance at high temperatures. The increment in capacity and stiffness and the analysis of the failure modes is the central focus of this paper. The experimental campaign is dealing with a significant number of un-reinforced and reinforced beams strengthened with unbonded GFRP plates. A 3-dimensional finite element model is also presented for simulating the non-linear behaviour of GFRP-reinforced softwood beams. The ability of the numerical model to reproduce experimental results for the load-deflection curves is validated.

Keywords: GFRP plates, softwood, screwed connection, composite materials, bending tests, FEM analysis.

1. INTRODUCTION

Softwood is from gymnosperm plants and it is the basis of approx. 85 % of the world's production of wood elements. Softwood as a traditional building material has been extensively used from antiquity to the present and, among softwoods, fir wood is characterised by low weight density and good performance in terms of tensile strength, is likely to distort during seasoning. Knots or grain deviation are the main causes of tension failures. Timber construction constitutes a significant part of the infrastructure in many countries: its extensive use is essentially due to its excellent workability, good mechanical

properties and low weight density. Splits caused during seasoning and natural defects may highly affect its mechanical properties and particularly cause high decreases of capacity. This reduction of the tensile strength may be as high as 90 % [1].

Softwood beams are usually replaced or reinforced with traditional methods involving the use of standard building materials such as steel or aluminum plates, or composite materials. Timber reinforcement is often necessary for civil infrastructures: approx.47 % of US timber bridges is structurally deficient according to the National Bridge Inventory [2].

The application of composites for strengthening of softwood beams is not new. FRPs (*Fiber Reinforced Polymers*) have high tensile strength and stiffness. The structural use of Glass and Carbon FRP composites (GFRP and CFRP, respectively) is becoming common not only for new timber members, but also for reinforcement of structural elements belonging to the architectural heritage. Composites are usually used where at least two of their beneficial properties, e.g. high tensile strength and ease of application, may be exploited. In these situations, the total cost of using composite materials is similar to metallic alternatives such as steel and aluminum plates or replacement.

There are three “traditional” methods for reinforcing timber beams with FRPs: 1) Bonding of consolidated (pultruded) laminates [3-5]; 2) Resin infusion of fabric reinforcement into grooves cut in the wood [6-11]; and 3) Wet lay up of FRP sheet reinforcement using epoxy adhesives [12-15]. According to the above procedures in the last two decades, FRP composites have been diffusively used in bridge decks, trusses, timber floors, etc. [16-19].

However the wide choice of composite products and their scattered mechanical properties can lead to serious problems for the designer. The selection of the reinforcement layout and the most appropriate material should be based on an accurate examination of the timber beams to be strengthened in order to avoid ineffective interventions [20-21]. The long-term durability of some FRPs also needs to be demonstrated [22-23].

Important issues remain to be solved. For example the use of FRP composites to reinforce timber beams without organic oil-based adhesives (e.g. epoxy resins) is less established. Recently, the use of natural fibres with non-organic matrixes or mechanical metal connectors has been investigated [24], and it aims at developing an interesting competitor to the use of organic oil-based fibres (e.g. CFRP) or resins, which present problems of limited durability, low reversibility and poor performance at high temperatures [25]. Governmental and local conservation bodies do not often authorize an extensive use of organic adhesives on listed timber structures and this highly limits the use of composite materials on historic constructions. Ethical guidelines for conservation works on historic constructions often list the minimal intervention and the use of appropriate materials and fully-reversible methods [26].

In the field of green building, there are several positive aspects in this research. For example, any disposal process requires sorting materials based on composition and nature and, because timber is doubtless the ultimate green building material, its preservation and use is also desirable [27].

The reinforcement method proposed in this research meets the above requirements. The results of flexure tests on firwood beams reinforced using GFRP plates, applied on the tension side without the use of an organic adhesive, are presented in this paper. Plates have been fixed to the beam's tension surface using metal screws or bolts [28-29]. Reinforcement can be easily removed, if needed, because no organic adhesives have been used for the application of the GFRP plates.

2. MATERIAL CHARACTERIZATION

2.1 Timber

A total of 41 sharp-edged softwood beams were tested of which 28 beams were reinforced with varying amounts of tensile reinforcement. The type of softwood used in the investigation is fir wood (*Abies Alba*). The wood stock was firstly assessed by visual and mechanical grading. Bending tests were conducted on beams with two different dimensions: 95x95x2000 mm (26 beams) and 200x200x4000 mm (15 beams) (Fig. 1). Small beams are composed of solid softwood while large beams are made of laminated timber, also called, glulam. For small beams the moisture content and weight density were 14.31 % (SD = 0.89 %) and 417 kg/m^3 (standard deviation SD = 24 kg/m^3), respectively. European standard EN 13183-1 [30] was used to measure the moisture content. For large beams moisture content and weight density were 11.31 % (SD = 0.37 %) and 430.8 kg/m^3 (SD = 18 kg/m^3), respectively.

The mechanical properties of timber in terms of Young's modulus and compressive strength are presented in Table 1. The compressive strength varied in the range of 34.54 to 40.43 MPa, and the Young's modulus from 9.54 to 11.91 GPa.

2.2 GFRP plate

The GFRP plates consisted in high-volume fraction high-strength unidirectional glass fiber in a polyester resin. Plates are produced by *Fibrenet SpA* under the commercial name of *Fbprofile*. The producer data sheet reports a Young's modulus and compressive strength of 32.6 GPa and 395 MPa, respectively. Results of mechanical characterization basically confirmed these values: according to ASTM D 3039 [31] standard Young's modulus was 31.57 GPa (SD = 2.458 GPa) with a tensile strength of 368.8 MPa (SD = 30.1 MPa). The manufacture of the GFRP plate is by pultrusion process (Tab. 2).

For small softwood beams, GFRP plates were reduced to a length of 1400 mm and were symmetrically applied on the beam's tension side using different types of steel screws. These beams were reinforced with a single GFRP pre-drilled plate (Fig. 2).

For reinforcement of large beams, two overlapping pre-drilled rectangular plates of dimensions 3600 × 80 × 9.5 mm (length × width × height) were used. GFRP plates were epoxy glued together and connected to the timber surface using metal screws or bolts. The mechanical properties of these plates are the same of the ones used for reinforcement of small beams.

3. EXTERNAL STRENGTHENING

Strengthening was performed with the application of the GFRP plates before the bending loads were applied. The timber surface was cleaned by air jet to rid it of loose particles and dust. The adhering face of the GFRP plate was also cleaned by acetone. Pre-drilled GFRP plates were fixed to the timber surface using commercially available metal screws (Fig. 3a) applied according to different configurations.

For the geometrical arrangement of the screws on small beams, four configurations have been used. According to the first arrangement, (Fig. 4a), 28 woodscrews (50 mm length, thread diameter 4 mm) were transversally placed at a centre-to-centre distance of 100 mm. All screws were positioned 25 mm from plate's edges. According to the second arrangement (Fig. 4b), 28 screws of the same type were placed diagonally (45°) at a centre-to-centre distance of 100 mm. Two or four U-shaped steel brackets have been used to increase the efficiency of the connection (3rd and 4th arrangement, respectively, Fig. 4c,d). The GFRP plate was epoxy glued to the steel bracket (Fig. 5).

For large beams, 8 mm-diameter metal screws or 18 mm-diameter bolts were used (80 and 100 mm in length, respectively). Three arrangements were adopted as shown in Figure 5. According to the first configuration (5th arrangement) 8 8mm-diameter (length = 80 mm) screws were applied (Fig. 5a). Screws have been placed at a centre-to-centre distance of 200 mm. For the second configuration (6th screw arrangement), 6 8mm-diameter (length = 100

mm) screws were used for each plate end, for a total of 12 screws (Fig. 5b). The last configuration (7th screw arrangement) is similar to first one: 6 18mm-diameter metal bolts were used (Fig. 5c). For all arrangements, screws or bolts were positioned 50 mm from GFRP plate's edge.

With the aim of comparing the effectiveness of the reinforcement technique, a limited number of both small and large softwood beams were strengthened by bonding the GFRP plate using an epoxy-resin. By ensuring perfect adherence between GFRP plate and timber, it was possible to define an upper limit to the capacity of reinforced beams.

Finally, for a small number of beams, steel brackets (Figs. 6 and 7) were used to increase the level of connection between and timber material and the GFRP plate. For each beam, 2 steel brackets were applied near the supports where the shearing force reaches the maximum value. GFRP plate was epoxy-glued to the internal surface of the steel brackets and by drilling holes on them it was possible to apply a larger number of metal screws. The aim was to cause a better distribution of the shear loads and a reduction of stress concentration around the holes and of slippage between the GFRP and timber (Figs. 8 and 9).

3. SHEAR CONNECTORS

In this investigation the connection between the softwood beams and the composite plates was done using commercially available woodscrews or bolts. The natural consequence of this connection is the shear flow between the two structural components. If there is no connection or the connectors fail, the softwood beam and the GFRP plate would bend and slip reciprocally. The presence of a shear connection prevents slippage between the two materials and provides the means to achieve the reinforcement action, thus increasing both flexural strength and stiffness of softwood beams. If perfect bonding (zero slip) occurs the two components behave as one and the effect of the reinforcement is maximum.

Because the four point bending test was used for both small and large beams, the longitudinal shear forces V_{AB} and V_{CD} are constant between the end-supports and the loading points:

$$V_{AB} = -V_{CD} = \frac{P}{2} \quad (1)$$

where P is the total value of the bending force applied.

Using the elastic theory of the beam, because normal strains and stresses vary linearly from the neutral axis to the extreme tension or compression fibre, the shear flow P_{Sd} at any level of a generic cross-section is:

$$P_{Sd} = \frac{V_{AD} Q^*}{I_{id}} \times i \quad (2)$$

where Q^* is the first moment about the neutral axis, I_{id} is the second moment of area of the effective cross-section of the reinforced beam and i is the centre-to-centre distance between two shear connectors. For both I_{id} and Q^* the area of the GFRP plate was taken as its transformed area using a modular ratio of 4.55.

By using and adapting the formulation given in Eurocode 4 for design of composite steel and concrete structures [32], the resistance of the shear connector is the smallest of the following:

$$P_{Rd} = 0.8 f_u \frac{\frac{\pi d^2}{4}}{\gamma_V} \quad (3)$$

$$P_{Rd} = 0.29 \times \alpha \times d^2 \frac{\sqrt{(f_{kw} \times E_w)}}{\gamma_V} \quad (4)$$

where f_u is steel connector's ultimate tensile strength, d is the diameter of the shear connector, γ_V is a partial factor for design shear resistance (usually 1.25), f_{kw} and E_w are the ultimate (parallel to grain) compression strength and Young's modulus of wood, respectively.

Eq. (3) derives from the design of shear connectors in concrete and it is used to study the effect of embedment of the connector. According to this theory:

$$\begin{cases} \alpha = 0.2\left[\left(\frac{h}{d}\right)+1\right] & if \quad 3 \le \frac{h}{d} \le 4 \\ \alpha = 1 & if \quad \frac{h}{d} > 4 \end{cases} \quad (5)$$

where h is the height of the shear connector. The total number of shear connectors needed is:

$$n_p = \frac{V_{AB}}{P_{Rd}} \quad (6)$$

The above theory has been used to estimate the needed number of connectors and it is based on the maximum shearing force values calculated by increasing of 50 % the maximum bending forces applied on un-reinforced beams. However clear limitations are present in this theory, making its application questionable and only possible for a preliminary design. The main limitations are:

1) The above formulas are based on the elastic theory of bending. This is acceptable for the GFRP plate, but not for timber. Non-linearity can occur (especially for low-grade timber) in wood due to yielding on the compression side. This will cause a shift of the neutral axis toward the compression side, a significant increment in deflections and shear flow.
2) The effectiveness of the reinforcement mainly depends on the bonding properties between the GFRP plate and the softwood beam and not on the resistance of the shear connector. Small values of slip may compromise the reinforcement's effectiveness.

3. METHODOLOGY AND TEST RESULTS

Four series of flexure tests were performed on unreinforced and reinforced beams (Tab. 3). It was decided to undertake four point bending tests, according to UNI EN 408 standard [33]. For small beams, a distance between the loading heads of 576 mm and a span of 1728 mm were used. In order to minimize local wood crushing, the beams were subjected to a double-point loading using two 42 mm-diameter steel cylinders by means of a compression hydraulic jack.

The simply-supported large softwood beams were monotonically loaded over a span of 3900 mm in four-point bending until failure occurred. A spreader steel H-shaped beam was used to apply the load to the beams, 1040 mm apart. Lateral supports were also used to preclude the lateral buckling of the beams. A load cell inside the 500 kN hydraulic actuator recorded the applied load.

For both small and large softwood beams, three inductive transducers (LVDT) were used to measure deflection at ¼, midspan and ¾ of the span. LVDT transducers were installed near the neutral axis (approx. the centre of the beam's height). Displacement-controlled loading with a crosshead speed of 2 mm/min was used.

The bending strength f_m was calculated according to:

$$f_m = a\frac{P_{\max}}{2W} \tag{7}$$

where P_{max} is the maximum value of the load; a is the distance between a loading head and the nearest end support (576 and 1430 mm, respectively for small and large beams) W is the modulus of resistance of the section (142.9 and 1333 cm^3). The global modulus of elasticity was calculated with the following equation:

$$E_{m,g} = \frac{l^3\left(P_2 - P_1\right)}{bh^3\left(d_2 - d_1\right)}\left[\left(\frac{3a}{4l}\right) - \left(\frac{a}{l}\right)^3\right] \tag{8}$$

where b is width of softwood beam cross section, l is the beam's span; $P_2 - P_1$ is an increment of the bending load on a straight-line portion of the load vs deflections response curve; d_2-d_1 is the deflection increment corresponding to $P_2 - P_1$.

The beams' stiffness k_1 and k_2, measured in the elastic range and at maximum load, respectively, was measured with the following:

$$\begin{cases} k_1 = \dfrac{\left(P_E - P_i\right)}{\left(d_{P_E} - d_{P_i}\right)} \\ k_2 = \dfrac{\left(P_{\max} - P_i\right)}{\left(d_{P_{\max}} - d_{P_i}\right)} \end{cases} \tag{9}$$

where P_E was 7 and 50 kN, for small and large softwood beams, respectively. P_i was a preload, applied to remove non-linear effects from the calculation of the beam's stiffness, of 2 and 5 kN, for small and large beams. d_{P_E} and d_{P_i} are the corresponding mid-span deflections at P_E and P_i.

Effect of reinforcement and post-elastic behavior were analyzed using the following indices:

$$\begin{cases} \delta_1 = \dfrac{P_{\max}}{P_{\max\, un}} \\ \delta_2 = \dfrac{d_{P_{\max}}}{d_{P_{\max\, un}}} \\ \delta_3 = \dfrac{k_1}{k_{1,un}} \end{cases} \tag{10}$$

$$\lambda = \frac{k_2}{k_1} \tag{11}$$

where $P_{\max,un}$, $d_{P_{\max,un}}$ and $k_{1,un}$ are the mean maximum load, the corresponding mid-span vertical deflection and stiffness measured for un-reinforced beams.

For small beams, the test setup is shown in detail in Figure 10.

3.1 Un-reinforced beams

For small beams, ten un-reinforced elements were subjected to flexure in four-point-bending. Load was applied incrementally until failure. Test results on unreinforced beams were used to evaluate the reinforcement's effectiveness through a comparison with the results of identical tests performed on small reinforced beams. For all specimens without reinforcement the letter designation used is UNS and UNL, for small and large beams respectively. For unreinforced beams different modes of fracture on the tension side were recorded: knot influenced, simple tension, cross grain tension (Fig. 11). Grain deviation or the presence of knots greatly influenced the crack propagation. Results of flexure tests on un-reinforced beams are shown in Table 4. The mean bending strength was 23.91 MPa (SD = 7.86 MPa) and the Young's

modulus $E_{m,g}$ 5932 MPa (dev. 907 MPa). In terms of capacity, the mean maximum load applied P_{max} was 11.86 kN and the corresponding mid-span deflection d_{Pmax} was 31.67 mm. The Coefficient of Variation (CoV) of the beam capacity is very high (CoV=32.8 %). Load-displacement response (Fig. 12) is initially linear. As the bending load increases, softwood begins to yield in compression and cracking occurs on the tension side. Beams UNS_2, UNS_4 and UNS_10 failed at a low load level due to the presence of a large defect (knot) on the tension side. For unreinforced beams, standard deviation (SD) of results in terms of capacity load was very high for the influence caused by the presence of natural timber defects.

Because of large softwood beams are made of glulam, the quantity and influence of defects is smaller compared to solid wood beams. This caused an increase of the mechanical properties (tensile strength and Young's modulus) and a reduction of the CoV. The mean capacity and bending strength was 71.87 kN (SD = 14.58 kN) and 38.54 MPa (SD = 7.82 MPa). The CoV was equal to 20.28 %. The crack usually ran horizontally along the grain and vertically between the load points where the bending moment is maximum.

The un-reinforced small and large softwood beams exhibited almost linear elastic behavior with brittle tensile failure. A very limited deviation from the value of 1 was calculated for the coefficient λ, given by the ratio between the stiffness in an elastic range and at maximum load (λ=1 denotes no variation in stiffness during loading and a perfect linear elastic behavior). For small and large beams, the value of λ was 0.812 and 0.88, respectively.

3.2 GFRP reinforced beams

3.2.1 Small softwood beams

Reinforced beams were tested with the same test procedure used for unreinforced ones. For each of the 16 small beam tests, graphs of mid-span deflection versus vertical load have been

drawn. These are presented in Figure 12. Numerical results are reported in Tables 5 and 6. For screw arrangement No.1 and 2, it can be seen that the measured ultimate (maximum) load increased significantly after the application of the GFRP reinforcement, with an increment in capacity of 59.9 and 58.9 %, respectively. The different orientation of the screws (vertical in Arrangement No. 1, and diagonal in Arrangement No. 2) did not cause a significant variation of the beam capacity and in its increment. The failure began with the displacement of the fasteners (screws) and of timber material. This caused a progressive loss of effectiveness of the GFRP reinforcement due to the slippage phenomena between the two materials.

By comparing the reinforced beams with control beams, it can be seen that the load at which the beams failed was not much higher for the reinforced beams, suggesting that the internal forces were only little shared between the GFRP plate and the timber. The use of an epoxy resin to bond the GFRP reinforcement caused a higher increase in beam capacity (+126 %) and demonstrated the importance to achieve a perfect bonding between the two materials. The load deflection plot is shown for beams reinforced with epoxy-glued and screwed GFRP plates in Figure 13. The composite action of the epoxy-glued GFRPs can be clearly seen here in the form of elevated stiffness (slope in the linear-elastic phase) and maximum bending load (beam's capacity). It is evident that the use of an epoxy resin is more reliable that the mechanical fasteners because it causes an higher increase in both stiffness and capacity. However the long term behavior of an epoxy bond should be investigated.

In order to prevent the displacement of the fasteners and/or of timber, steel brackets have been applied near the supports to facilitate the transmission of the internal shearing force between the timber and the GFRP reinforcement. The most part of these timber beams failed because of timber cracking on the tension side; it was also observed that GFRP plates did not crack. For this reason a residual bending strength has been detected following timber failure. The beams reinforced according to the 3rd arrangement (2 steel brackets) evidenced an average

bending capacity of 18.79 kN, with an increment of 58.4 % compared to unreinforced beams. However by comparing this value with the result of small beams reinforced without the use of steel brackets a negligible increase of the bending strength has been recorded.

Finally the application of 4 steel brackets according to the 4th Arrangement produced a significant increase of both the bending strength (75.1 %) and mid-span deflection at maximum load (316.6 %) compared with control beams.

An important consequence of the application of the GFRP reinforcement is the increment in the beams's stiffness, measured using the coefficient δ_3 in equation (10). Values of δ_3, varying between 40.2 and 98.9 %, have been measured for small beams reinforced according to the four configurations. It is worth to compare these values of δ_3 with the ones calculated for beams reinforced using an epoxy resin to bond the GFRP plates. The use of an epoxy resin allowed to achieve the condition of no-strain (zero-slippage) between the two materials (softwood and GFRP) and the maximum possible value of stiffness. This represents an upper bound of the stiffness value and its increment compared to control beams. Beams reinforced using an epoxy resin exhibited a stiffness of 1273 N/mm with an increment 181.8 % compared with control beams. On the other hand, beams reinforced using screwed connections exhibited values of the stiffness approx. 30-35 % smaller compared to this upper bond value denoting the above mentioned displacement phenomena of the fasteners.

The reinforced small softwood beams exhibited plastic elastic behavior with brittle tensile failure of timber material. A high deviation from the value of 1 was calculated for the coefficient λ. This coefficient varied between 0.317 (1st arrangement) and 0.653 (use of epoxy resin). The high deviation from the linear behavior in mainly produced by two causes: the displacement of the fasteners (screws) and of timber material and yielding phenomena of timber in compression. It is not easy to quantify the two causes: however the sole contribution of the wood yielding can be determined from the results of beams reinforced using an epoxy

resin: for these beams λ=0.653, denoting a significant contribution of the displacement phenomena of beams reinforced using screws (λ=0.317-0.486).

3.2.2 Large softwood beams

As expected, the application of the GFRP plate also increased the bending strength of large beams, but results highly differed depending on the arrangement, diameter and number of screws used. A summary of the test results, obtained from the four-point bending tests, is presented in Table 7 and Figure 14. Reference UNL denotes a test on an un-reinforced softwood beam while the reference REL is used for GFRP-reinforced beams.

The application of only 8 8mm-diameter screws (5th arrangement) did not cause an appreciable increment both in capacity (-0.04 %) and stiffness (5.7 %). The displacement of both the screws and timber material caused the detachment of the GFRP reinforcement and compromised its reinforcing action (Fig. 15).

By increasing the number of screws, the effectiveness of the reinforcement also increased, but very little. The application of GFRP plates according to the 6th screw arrangement (by using 12 8 mm-diameter screws) caused an increase of the beam's capacity δ_1 and stiffness δ_3 of 25.2 and 5.6 %, respectively. The failure again began with the displacement of the screws and of timber material, producing slippage phenomena that compromised the effectiveness of the reinforcement. All beams reinforced according to the 5th and 6th arrangements demonstrated tensile failures initiated by defects in the timber material. Results also indicate that the reinforcement produced an increment of the mid-span deflection δ_2 at maximum load between 4.1 and 27.6 %, compared to control un-reinforced beams (Tables 8 and 9).

By replacing screws with larger diameter bolts (diameter 18 mm, length 100 mm) it was possible to reduce the stresses both in the metal and in the bottom timber lamination (7th arrangement). Beams reinforced according to this arrangement exhibited a more linear elastic

behaviour caused by the reduction of the displacement phenomena in the area around the holes. Yielding of timber material in compression and the low bearing resistance at the joint bolt-timber produced a plastic behaviour for high values of the bending load. Failure was first produced by shear rupture of the metal bolts (Fig. 16) and subsequently timber cracking. All beams failed in the pure moment region (between the points of application of the bending loads). Photographs of typical fractures are shown in Figure 17.

By applying steel brackets near the lateral supports (Fig. 18), it was possible to increase the level of connection between the GFRP reinforcement and softwood. Two or four steel brackets were positioned approximately 200 mm inside the lateral supports. Each 2 mm-thick steel bracket was connected to the softwood beam using two 18 mm-diameter through bolts (Figs. 19 and 20) and one 18 mm-diameter 100 mm length bolt. The application of the GFRP reinforcement according to the 8^{th} arrangement (two steel brackets) produced an increase in the beam capacity δ_1 of 29 %. An increment of 31.1 % was recorded for the 9^{th} arrangement. The increment in stiffness δ_3 was similar for both these two reinforcement arrangement (25.6 and 25.3 %, respectively).

Similarly to the previous tests on small beams, for two large beams the GFRP plate was applied using an epoxy adhesive. This produced an increment of the beam capacity δ_1 and stiffness δ_3 of 42.7 and 41 %, respectively and it represents an upper bound for the reinforcement effectiveness (Fig. 21).

For tests REL_7 and REL_8 the strains of the GFRP plate were determined by one strain gauges (gage factor 2.05, resistance 120 W) applied in plate's centre at mid-span (1800 mm from the end of the GFRP plate). Gauge was placed parallel to the long plate axis. For test REL_7 (epoxy-bonded plate) a maximum strain of 0.554 % was measured. This generates in the plate a tensile stress of 174.9 MPa equal to 47.5 % of the plate tensile strength.

Conversely, strain data from REL_8 (screwed connection made with 12 8 mm-diameter

screws) show only a tensile stress 36.7 MPa. This low value is again the consequence of displacement phenomena producing slippage between softwood and GFRP plate.

4. NUMERICAL ANALYSIS

4.1 Model development

Non-linear static analysis has been carried out on a complete three-dimensional FE model of both unreinforced and FRP-reinforced softwood beams. Simulation was made using commercial software Ansys, ver. 15.0 [34]. The numerical model was built to accurately reproduce the geometry of the specimens. To this end, minor regularizations were made and the presence of imperfections was disregarded. The geometry of the timber beams were firstly reconstructed by means of CAD tools, next the volumes were imported and modelled using Solid45 elements (three dimensional eight-node hexahedron isoparametric elements), which are defined by eight nodes with three degrees of freedom at each node and orthotropic material properties. The average size of the hexahedron elements was chosen so as to have 10x10 elements across the specimen cross section: this allows the more critical details to be captured avoiding shear lock effects.

For the reinforcement, the Shell181 element was chosen to model the GFRP plate. This element material was also assumed to be orthotropic and the stress-strain relationship was assumed to be linear up to failure. GFRP plates were connected to joint points on the beam. The same mesh size was used to model the GFRP plate and softwood beam in order to provide full overlap at the joints. Figure 22 shows the finite element model consisting of 25,974 nodes and 25,360 elements, with 76,992 degrees of freedom.

Values concerning the physical properties of timber were established on statistical analysis of test data found in the literature [35] and from previous mechanical characterization. The final inputs had the following values: E_x = 10,500 MPa; E_y = 330 MPa; E_z = 330 MPa; υ_{xy} = 0.041;

υ_{yz} = 0.350; υ_{xz} = 0.033; G_{xy} = 630 MPa; G_{yz} = 630 MPa; G_{xz} = 630 MPa; ρ = 420 kgm^{-3}. A linear elastic response was assumed for the GFRP material, with the Young's modulus and the Poisson's ratio equal to 80 % of the experimentally measured values (Tab. 2), considering the variance of the results.

To increase the reliability of the proposed FEM, unilateral contact interfaces were used for the simulation of the contacts between the specimen and the loading plates and bearing supports, respectively. The modeling of the contacts requires the use of specific flexible/flexible elements. Specifically a unilateral contact law was applied in the normal direction of each interface, indicating that no tension forces can be transmitted in this direction and a gap may appear if the stresses become zero. For the behavior in the tangential direction, it was taken into account that sliding may or may not occur, by using the Coulomb friction model with a friction coefficient equal to 0.4.

4.1 Analysis results

In order to find the actual stress field at maximum load, a finite element analysis was conducted, in which the timber beams were subjected to both self-weight and a uniform load pressure under different load stages.

The results of the finite element analysis are summarized in Figure 23, showing the contour plots of the maximum principal stress (maximum tensile stress) on the tests specimens. To show the efficiency and accuracy of the proposed FEM model, the predictions of the ultimate load capacity are compared with experimental results in Table 10. This comparison reveals good agreement between the theoretical predictions and experimental data for the collapse mode and for the corresponding load-carrying capacity. The unreinforced beam was predicted to fail in tension in a brittle manner, as was also determined experimentally, and the deviations between the calculated and measured values

was found to be no more than 14 %. A good agreement between theoretical and experimental results was also detected for both epoxy-bonded and unbonded GFRP-reinforced beams. The error of the model was in fact 12 % in both cases. As for the failure mode (Fig. 24), the FEM model properly simulated the experimental behavior of the beams, which failed because of timber cracking on the tension side (suggesting that the internal forces were not completely shared between the GFRP plate and the timber).

5. CONCLUSIONS

The mechanical behavior of low-grade (softwood) solid and laminated (glulam) beams reinforced using unbonded pultruded GFRP plates has been investigated. The pultrusion process is ideally suited to the economic production of prismatic composite profiles and the GFRP application without polymeric adhesives may be of interest to avoid irreversible interventions and to guarantee a more durable mechanical connection between timber substrate and reinforcement. The composite plates were anchored at the bottom of softwood beams using metal screws or bolts.

The fastener's and timber displacement, induced by both the low quality of commercially available fasteners and the limited parallel-to-grain timber compression strength, partially compromised the effectiveness of the reinforcement. Different fasteners' configurations were investigated. In order to reduce the stress concentration near the connection, the fasteners' number and/or diameter was increased: in this way it was possible to achieve an increase of bending strength up to 58.9 % and of the flexural stiffness up to 98.9 %. A further increment in both capacity and stiffness was measured when steel brackets were applied near the beam's end-supports to increase the level of connection between GFRP plate and timber.

The typical failure mode of GFRP-reinforced beams initiated from the displacement of the metal fasteners and timber material and subsequently resulted in timber cracking on the

tension side without any significant damage to the GFRP plate. Strain measurements on the GFRP pultruded plates were always well below the plate's tensile strength.

The effectiveness of the reinforcement was studied by deriving an upper bound for capacity and stiffness (by preventing slippage between GFRP plate and softwood beams). This was achieved by using an epoxy adhesive to bond the two materials.

Initial prediction from the numerical model showed good agreement with test results for capacity, mid-span deflection and stiffness. However the modelling method of the connections between the metal fasteners and softwood needs to be further investigated in order to take into account the local effects in terms of shear stresses and displacements.

ACKNOWLEDGEMENTS

The authors acknowledge the support of the *Lastru* laboratory at the University of Perugia (Italy) for the use of the test equipment. This project was sponsored by the Italian Ministry of Education [ReLUIS (2014) Linea di ricerca WP1 e WP2].The investigation was carried out with the help of the undergraduate students G. Capruzzi, M. S. Bernardi and S. Rumori, and the graduate research assistant A. Molinari. The authors also express their gratitude to Fibrenet for providing the composite materials.

REFERENCES

[1] Thelandersson S, Larsen HJ. Timber engineering. John Wiley & Sons 2003.

[2] FHWA. US Department of Transportation, Seventh annual report to the congress on highway bridge replacement and rehabilitation program. 1986.

[3] Corradi M, Borri A. Fir and chestnut timber beams reinforced with GFRP pultruded elements. Compos Part B-Eng 2007;38, 172-181.

[4] Raftery GM, Harte AM. Low-grade glued laminated timber reinforced with FRP plate. Compos Part B-Eng 2011; 42(4), 724-735.

[5] Nowak TP, Jasieńko J, Czepiżak D. Experimental tests and numerical analysis of historic bent timber elements reinforced with CFRP strips. Constr Build Mater 2013; 40, 197-206.

[6] Chajes MJ, Kaliakin VN, Meyer AJ. Behaviour of engineered wood-CFRP beams. Proc., 5th Int. Conf. on Camp. In Infrastr., H. Saadatmanesh and M. R. Ehsani, eds., Univ. of Arizona, Tucson, Arizona, 1996; 870-877.

[7] Gentile C, Svecova D, Rizkalla SR. Timber beams strengthened with GFRP bars: development and applications. J Compos Constr 2002; 6, 11-20.

[8] Borri A, Corradi M, Grazini A. A method for flexural reinforcement of old wood beam with CFRP materials. Compos Part B-Eng 2005; 36, 143-153.

[9] Micelli F, Scialpi V, La Tegola A. Flexural reinforcement of glulam timber beams and joints with carbon fiber-reinforced polymer rods. J Compos Constr 2005; 9, 337-347.

[10] Raftery GM, Whelan C. Low-grade glued laminated timber beams reinforced using improved arrangements of bonded-in GFRP rods. Constr Build.Mater 2014; 52, 209-220.

[11] Righetti L, Corradi M, Borri A. Bond strength of vomposite CFRP reinforcing bars in timber. Materials 2015; 8, 4034-4049.

[12] Plevris N, Triantafillou TC. FRP-Reinforced Wood as structural material. J Mater Civ Eng 1992; 4, 300-317.

[13] Radford DW, Van Goethem D, Gutkowski RM, Peterson ML. Composite repair of timber structures. Constr Build Mater 2002; 16, 417-425.

[14] Hay S, Thiessen K, Svecova D, Bakht B. Effectiveness of GFRP sheets for shear strengthening of timber. J Compos Constr 2006; 10, 483-491.

[15] Schober KU, Harte AM, Kliger R, Jockwer R, Xu Q, Chen JF. FRP reinforcement of timber structures. Constr Build Mater 2015; 97, 106-118.

[16] Davanos JF, Zipfel MG, Quiao P. Feasibility study of prototype GFRP-reinforced wood railroad crosstie. J Compos Constr 1999; 3(2), 92-99.

[17] Lopez-Anido R, Hu H. Structural characterization of hybrid FRP-Glulam panels for bridge decks. J Compos Constr 2002; 6(3), 194-203.

[18] Jankowski LJ, Jasieńko J, Nowak TP. Experimental assessment of CFRP reinforced wooden beams by 4-point bending tests and photoelastic coating technique. Mater Struct 2010; 43(1-2), 141-150.

[19] Jasieńko J, Nowak TP, Bednarz Ł. Baroque structural ceiling over the Leopoldinum Auditorium in Wrocław University: tests, conservation, and a strengthening concept. Int J Archit Herit 2014; 8(2), 269-289.

[20] Tampone G. Il restauro delle strutture di legno. Hoepli Editore 1996 [in Italian].

[21] Sandanus J, Sogel . Refurbishment of Significant Timber Structures in Slovakia. Journal of Civil Engineering and Architecture 2014; 8(8).

[22] Tascioglu C, Goodell B, Lopez-Anido R, Peterson M, Halteman W, Jellison J. Monitoring fungal degradation of E-glass/phenolic fiber reinforced polymer (FRP) composites used in wood reinforcement. International Biodeterioration Biodegradation 2003; 51, 157-165.

[23] Borri A, Castori G, Corradi M, Speranzini E. Durability analysis for FRP and SRG composites in civil applications. Key Engineering Materials 2015; 624, 421-428.

[24] Borri A, Corradi M, Speranzini E. Reinforcement of wood with natural fibres. Compos Part B-Eng 2013; 53, 1-8.

[25] Papanicolaou CG, Triantafillou TC, Papathanasiou M, Karlos K. Textile reinforced mortar (TRM) versus FRP as strengthening material of URM walls: out-of-plane cyclic loading. Mater Struct 2008, 41, 143–57.

[26] Feilden B. Conservation of historic buildings. Routledge 2007.

[27] Wang L, Toppinen A, Juslin H. Use of wood in green building: a study of expert perspectives from the UK. J Clean Prod 2014; 65, 350-361.

[28] Blass HJ, Bejtka I. Reinforcements perpendicular to the grain using self-tapping screws. In The 8th World Conference on Timber Engineering, Lahti, Finland (Vol. 1) 2004.

[29] Munafò P, Stazi F, Tassi C, Davì F. Experimentation on historic timber trusses to identify repair techniques compliant with the original structural–constructive conception. Constr Build Mater 2015; 87, 54-66.

[30] EN 13183-1:2002. Moisture content of a piece of sawn timber. Determination by oven dry method.

[31] ASTM D3039:2009. Standard test method for tensile properties of fiber-resin composites.

[32] Eurocode 4, EN, C., 1994. 1-1, 2004. Design of composite steel and concrete structures. Part 1-1: General rules and rules for buildings.

[33] EN 408:2010. Timber structures. Structural timber and glued laminated timber: determination of some physical and mechanical properties.

[34] ANSYS Inc. AUTODYN user manual version 15; 2013.

[35] EN 338:2009. Structural timber - Strength classes.

Figure 1: a) Small softwood solid beams. b) Large softwood glulam beams

Figure 2: Application of a pre-drilled GFRP plate on small softwood beams.

Figure 3: Detail of the used fully threaded woodscrews for reinforcement a) length L=50 mm. diameter ϕ=4 mm; b) length L=100 mm. diameter ϕ=18 mm

Figure 4: Detail of the method of connection of the GFRP plate to the wood tension side (small beams): a) 28 trasversal screws (1st arrangement); b) 28 diagonal screws (2nd arrang.); c) 2 steel brackets and 20 trasversal screws (3rd arrang.); d) 4 steel brackets (4th arrang.) [dimensions in (mm)].

Figure 5: Detail of the method of connection of the GFRP plate to the wood tension side (large beams): a) No. 8 8mm-diameter screws (5th arrang.); b) No. 12 8mm-diameter screws (6th arrang.); c) No. 6 18mm-diameter screws (7th arrang.) [dimensions in (mm)].

Figure 6: The steel brackets used for reinforcement on small a) and large b) softwood beams.

Figure 7: Detail of the connection at a steel bracket.

Figure 8: The four small beams after the application of the reinforcement and of two steel bracktes.

Figure 9: Detail of the method of connection of the GFRP plate to the wood tension side (large beams): a) 2 steel brackets and 6 trasversal bolts (8th arrang.); b) 4 steel brackets and 6 trasversal bolts (9th arrang.) (dimensions in mm).

Figure 10: Small softwood beams: four-point bending.

Figure 11: Typical failure along the grain.

Figure 12: Load vs. mid-span displacement for unreinforced and reinforced small softwood beams.

Figure 13: Load vs. mid-span displacement for reinforced small softwood beams: epoxy-bonded reinforcement (black curves). screwed reinforcement (grey curves).

Table 1: Properties of the timber

	Small beams	Large beams
Wood species	*Abies Alba*	
Wood type	Solid	Glulam
Weight density (kg/m^3)	417 (24.2)	430.8 (18.2)
Moisture content (%)	14.31 (0.89)	11.31 (0.37)
Specimen dimensions (mm)	20x20x60	20x20x60
Number of tested specimens	10	10
Compressive strength (MPa)	36.90 (2.06)	37.94 (2.56)
Young's modulus (GPa)	10.55 (1.81)	11.9 (1.55)

SD in ( ).

Table 2: Properties of the GFRP plate.

Thickness (mm)	9.5
Sample size	10
Tensile strength (MPa)	368.8 (30.1)
Weigth density (kg/m^3)	1779 (51.8)
Young's modulus (MPa)	31575 (2458)
Strain at failure (%)	1.19

SD in ( ).

Table 3: Test matrix.

Index	Number of softwood beams	Reinforcement
UNS_series	10	Un-reinforced
RES_series	16	GFRP plate
UNL_series	3	Un-reinforced
REL_series	12	GFRP plate

Table 4: Test results (small beams).

Index	Connection Timber-Plate	Maximum load P_{max} (kN)		Bending strength f_m (MPa)	Deflection at maximum load d_{Pmax} (mm)	
UNS_1	-	12.92		26.04	38.5	
UNS_2	-	7.44		14.99	23.49	
UNS_3	-	14.70		29.63	36.65	
UNS_4	-	8.41		16.95	22.70	
UNS_5	-	14.25	11.86	28.72	42.90	31.67
UNS_6	-	12.91	(3.90)	26.02	36.30	(9.59)
UNS_7	-	15.76		31.76	41.60	
UNS_8	-	15.38		31.00	32.60	
UNS_9	-	12.78		25.76	29.20	
UNS_10	-	4.06		8.18	12.80	
RES_11	28 screws	18.41		37.10	43.88	
RES_12	L=50mm,	14.66	18.96	29.55	32.47	44.55
RES_15	ϕ=4mm	23.81	(4.60)	47.99	57.31	(12.43)
RES_13	28 screws*	15.38		31.00	26.90	
RES_14	L=50mm,	22.15	18.84	44.64	45.81	34.92
RES_16	ϕ=4mm	19.00	(3.39)	38.29	32.05	(9.78)
RES_17	4 steel	17.91		36.10	26.25	
RES_18	brackets	26.13	20.77	52.66	79.72	49.51
RES_19		18.52	(3.74)	37.33	61.56	(25.66)
RES_20		20.50		41.32	30.12	
RES_21	2 steel	15.88		32.01	22.57	
RES_22	brackets +	19.45	18.79	39.20	37.29	31.63
RES_23	20 screws	13.05	(5.93)	26.30	26.59	(8.38)
RES_24	L=50mm	26.76		53.93	40.06	
RES_25	Epoxy	25.13	26.76	50.65	20.06	22.89
RES_26		28.39	(2.31)	57.22	25.72	(4.00)

* applied diagonally, SD in ( ).

Table 5: Effect of reinforcement (small beams).

	Number of tested beams	Maximum load P_{max} (kN)	$\delta_1 = \frac{P_{\max}}{P_{\max\ un}}$ (-)	Deflection at maximum load d_{Pmax} (mm)	$\delta_2 = \frac{d_{P_{\max}}}{d_{P_{\max\ un}}}$ (-)
Unreinforced	10	11.86		31.67	
1st Arrangement	3	18.96	1.599	44.55	1.407
2nd Arrangement	3	18.84	1.589	34.92	2.944
3rd Arrangement	4	18.79	1.584	31.63	2.667
4th Arrangement	4	20.77	1.751	49.41	4.166
Epoxy resin	2	26.76	2.256	22.89	1.930

Table 6: Stiffness properties of reinforced and unreinforced small beams.

	Number of tested beams	k_1 (N/mm)		$\delta_3 = \frac{k_1}{k_{1,un}}$ (-)	k_2 (N/mm)		$\lambda = \frac{k_2}{k_1}$ (-)
Unreinforced	10	451.6	(85.8)	-	366.6	(54.8)	0.812
1st Arrangement	3	633.1	(185.8)	1.402	200.8	(63.6)	0.317
2nd Arrangement	3	898.1	(284.1)	1.989	279.7	(67.0)	0.311
3rd Arrangement	4	861.5	(300.7)	1.908	418.5	(74.5)	0.486
4th Arrangement	4	745.0	(233.9)	1.650	252.4	(108.3)	0.339
Epoxy resin	2	1273	(212.1)	2.818	831.3	(12.9)	0.653

SD in ( ).

Table 7: Test results (large beams).

Index	Connection Timber-Plate	Maximum load P_{max} (kN)		Bending strength f_m (MPa)	Deflection at maximum load d_{Pmax} (mm)	
UNL_1	-	59.39		31.85	44.95	
UNL_2	-	68.32	71.87	36.64	55.88	62.12
UNL_3	-	87.89	(14.58)	47.13	85.54	(21.00)
REL_4	8 screws L=80mm	74.64	71.59	40.03	68.69	64.70
REL_5	ϕ=8mm	68.53	(4.32)	36.75	60.71	(5.64)
REL_6	Epoxy	82.52	102.52	44.25	78.61	95.13
REL_7		122.52	(28.28)	65.70	111.65	(23.36)
REL_8	12 screws L=100mm	80.92	89.99	43.39	66.37	79.27
REL_9	ϕ=8mm	99.06	(12.83)	53.12	92.17	(18.24)
REL_10	6 screws L=100mm	93.26	89.74	50.01	73.15	69.69
REL_11	ϕ=18mm	86.22	(4.98)	46.24	66.23	(4.89)
REL_12	6 screws L=100mm	116.87	92.73	62.67	105.84	75.94
REL_13	ϕ=18mm+2 brackets	68.59	(34.14)	36.78	46.04	42.28
REL_14	6 screws L=100mm	93.37	95.64	50.07	64.97	69.29
REL_15	ϕ=18mm+4 brackets	97.90	(3.20)	52.50	73.6	(6.10)

SD in ( ).

Table 8: Effect of reinforcement (large beams).

	Number of tested beams	Maximum load P_{max} (kN)	$\delta_1 = \frac{P_{\max}}{P_{\max\ un}}$ (-)	Deflection at maximum load d_{Pmax} (mm)	$\delta_2 = \frac{d_{P_{\max}}}{d_{P_{\max\ un}}}$ (-)
Unreinforced	3	71.87		62.12	
5th Arrangement	2	71.59	0.996	64.70	1.041
6th Arrangement	2	89.99	1.252	79.27	1.276
7th Arrangement	2	89.74	1.249	69.69	1.122
8th Arrangement	2	92.73	1.290	75.94	1.222
9th Arrangement	2	95.64	1.331	69.29	1.115
Epoxy resin	2	102.5	1.427	95.13	1.531

Table 9: Stiffness properties of reinforced and unreinforced large beams.

	Number of tested beams	k_1 (N/mm)		$\delta_3 = \frac{k_1}{k_{1,un}}$ (-)	k_2 (N/mm)		$\lambda = \frac{k_2}{k_1}$ (-)
Unreinforced	3	1202	(25.84)	-	1058	(239.7)	0.880
5th Arrangement	2	1270	(62.30)	1.057	1144	(82.52)	0.901
6th Arrangement	2	1269	(26.66)	1.056	1146	(111.9)	0.904
7th Arrangement	2	1367	(32.53)	1.137	1286	(27.79)	0.941
8th Arrangement	2	1510	(43.49)	1.256	1261	(253.3)	0.835
9th Arrangement	2	1506	(70.29)	1.253	1356	(59.82)	0.901
Epoxy resin	2	1695	(145.6)	1.410	1070	(29.27)	0.631

SD in ( ).

Table 10: Experimental versus predicted ultimate load capacities.

	Experimental load capacity ($P_{max,ex}$) (kN)	Predicted load capacity ($P_{max,th}$) (kN)	$\frac{P_{max,ex}}{P_{max,th}}$
Unreinforced	11.86	13.80	0.86
1st Arrangement	18.96	17.00	1.12
Epoxy resin	26.76	24.00	1.12

a) b)

Figure 1: a) Small softwood solid beams. b) Large softwood glulam beams

Figure 2: Application of a pre-drilled GFRP plate on small softwood beams.

a)

b)

Figure 3: Detail of the used fully threaded woodscrews for reinforcement a) length L=50 mm. diameter ϕ=4 mm; b) length L=100 mm. diameter ϕ=18 mm

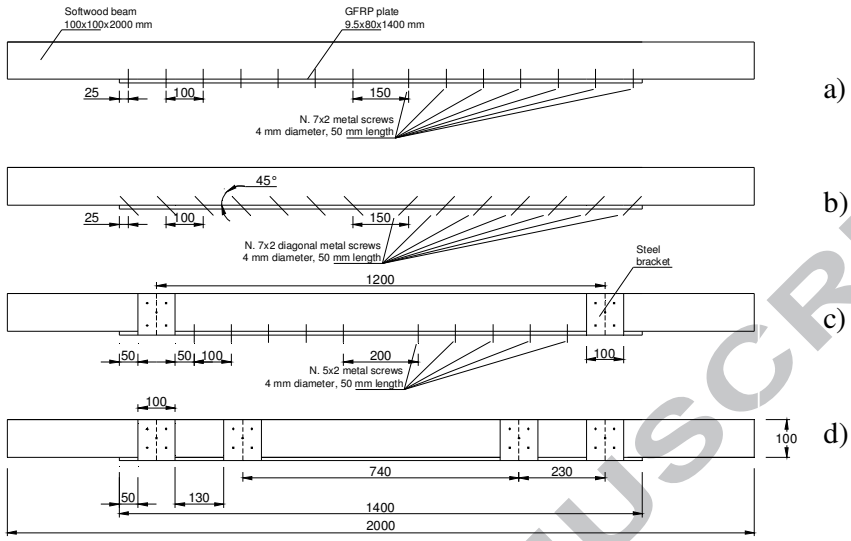

Figure 4: Detail of the method of connection of the GFRP plate to the wood tension side (small beams): a) 28 trasversal screws (1st arrangement); b) 28 diagonal screws (2nd arrang.); c) 2 steel brackets and 20 trasversal screws (3rd arrang.); d) 4 steel brackets (4th arrang.) [dimensions in (mm)].

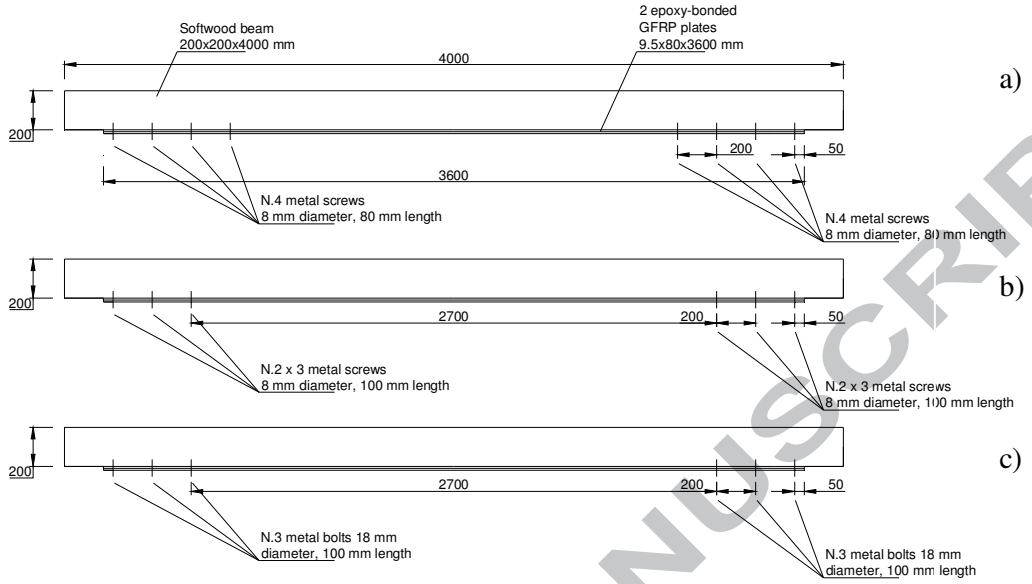

Figure 5: Detail of the method of connection of the GFRP plate to the wood tension side (large beams): a) No. 8 8mm-diameter screws (5^{th} arrang.); b) No. 12 8mm-diameter screws (6^{th} arrang.); c) No. 6 18mm-diameter screws (7^{th} arrang.) [dimensions in (mm)].

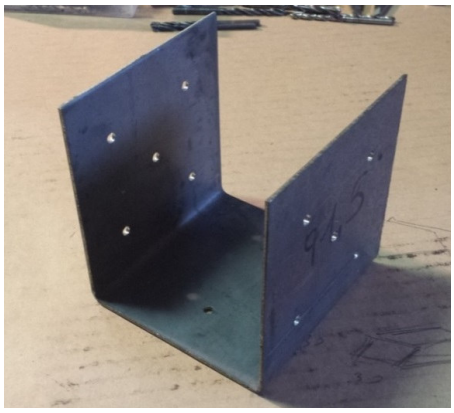
a)


b)

Figure 6: The steel brackets used for reinforcement on small a) and large b) softwood beams.

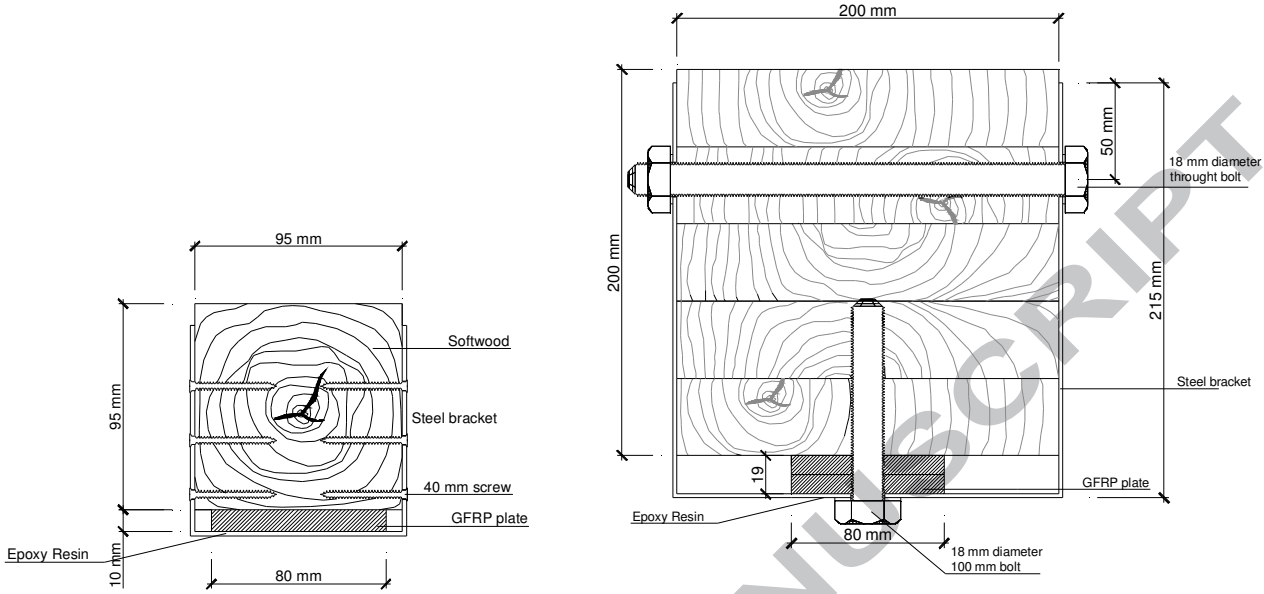

Figure 7: Detail of the connection at a steel bracket.

Figure 8: The four small beams after the application of the reinforcement and of two steel bracktes.

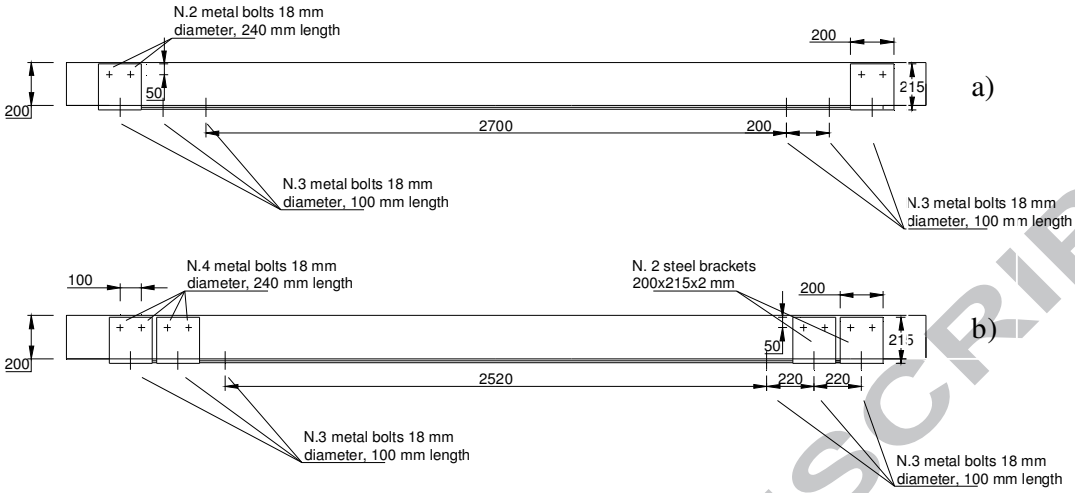

Figure 9: Detail of the method of connection of the GFRP plate to the wood tension side (large beams): a) 2 steel brackets and 6 trasversal bolts (8^{th} arrang.); b) 4 steel brackets and 6 trasversal bolts (9^{th} arrang.) (dimensions in mm).

Figure 10: Small softwood beams: four-point bending.

Figure 11: Typical failure along the grain.

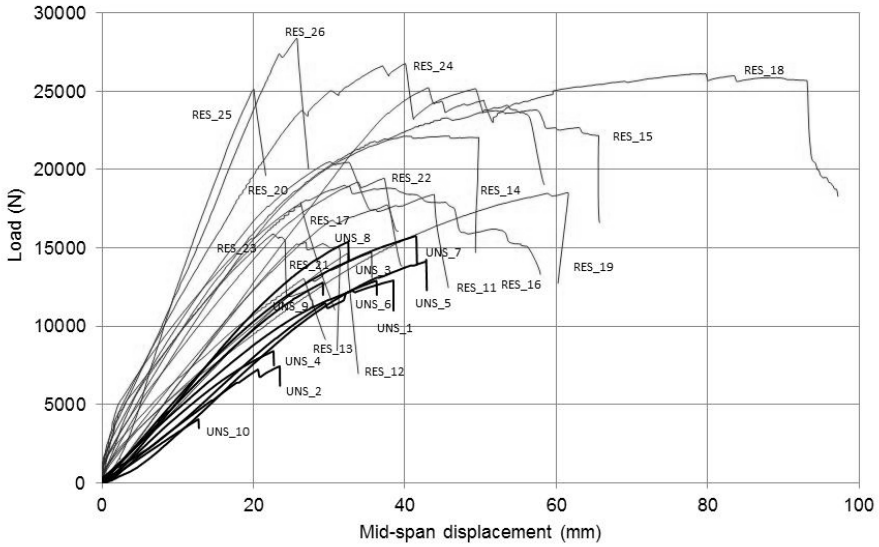

Figure 12: Load vs. mid-span displacement for unreinforced and reinforced small softwood beams.

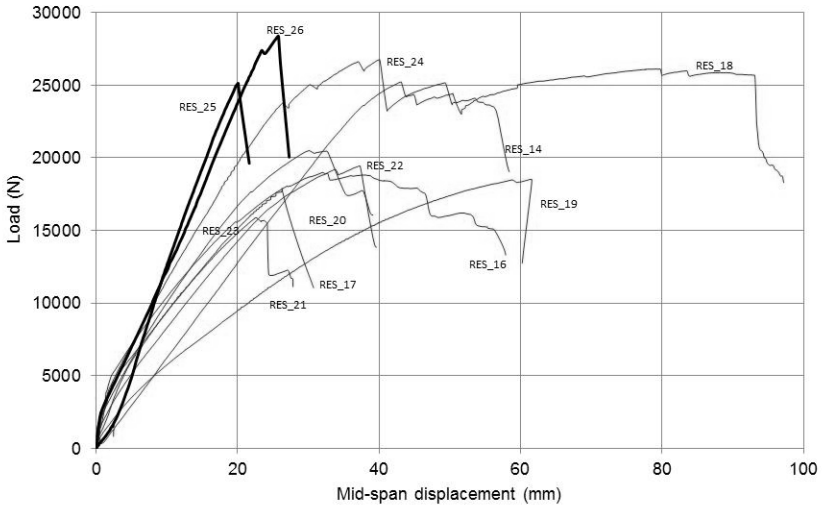

Figure 13: Load vs. mid-span displacement for reinforced small softwood beams: epoxy-bonded reinforcement (black curves). screwed reinforcement (grey curves).

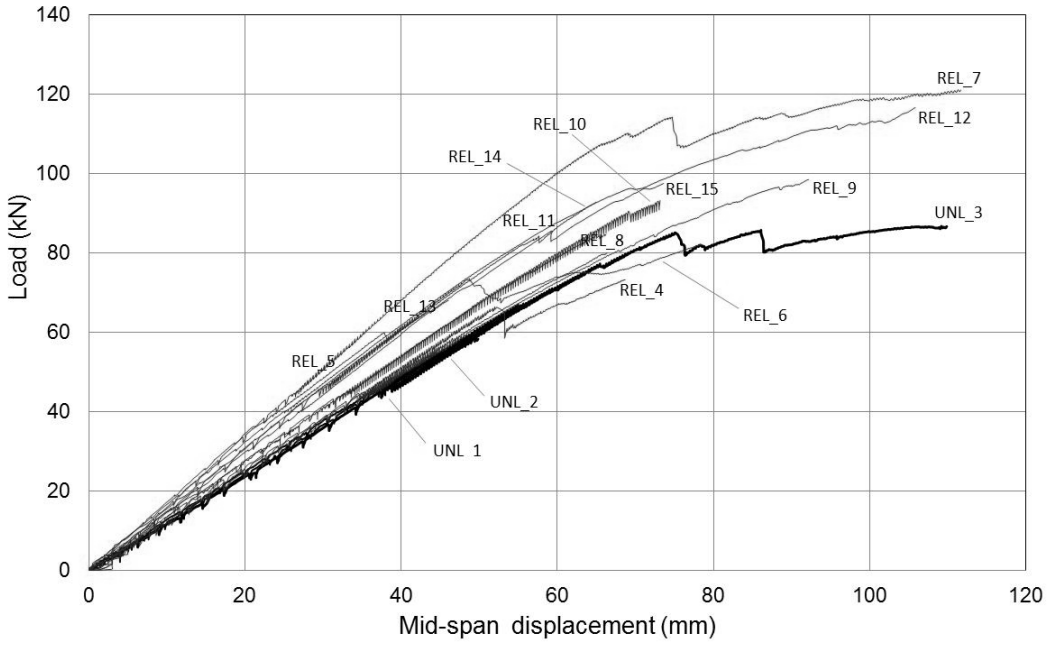

Figure 14: Load vs. mid-span displacement for unreinforced and reinforced large softwood beams.

Figure 15: Detail of the displacement of the metal 8 mm-diameter screws (5th arrangement).

Figure 16: Shear failure of metal bolts (7th arrangement).

Figure 17: Detail of tensile failure in timber.

Figure 18: Detail of the steel brackets applied on large beams.

Figure 19: 18 mm-diameter steel though bolts used to connect the steel bracket with softwood beams.

Figure 20: 4-point bending test on a GFRP reinforced beam (with steel brackets).

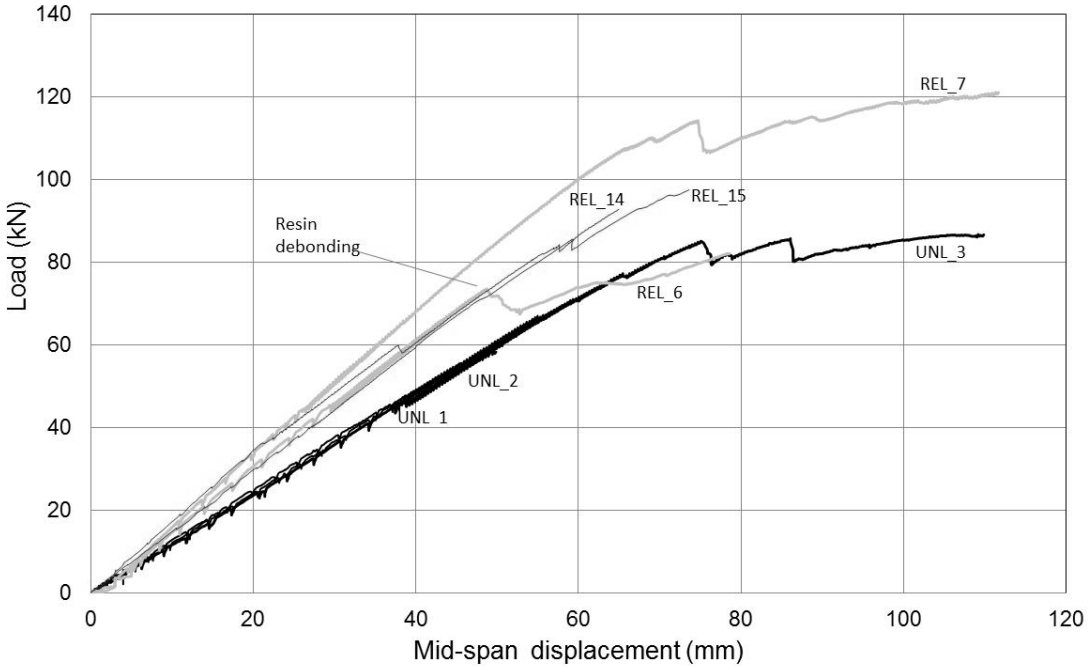

Figure 21: Load vs. mid-span displacement for reinforced large softwood beams: epoxy-bonded reinforcement (bold grey curves), screwed reinforcement (grey curves), unreinforced beams (black curves).

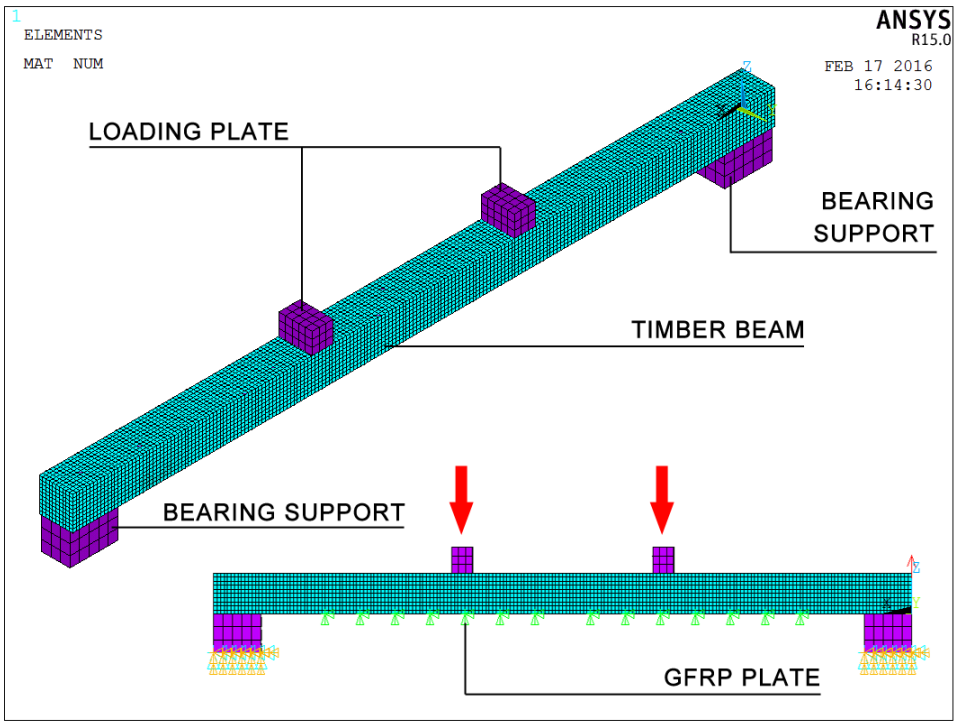

Figure 22: FEM model: mesh discretization.

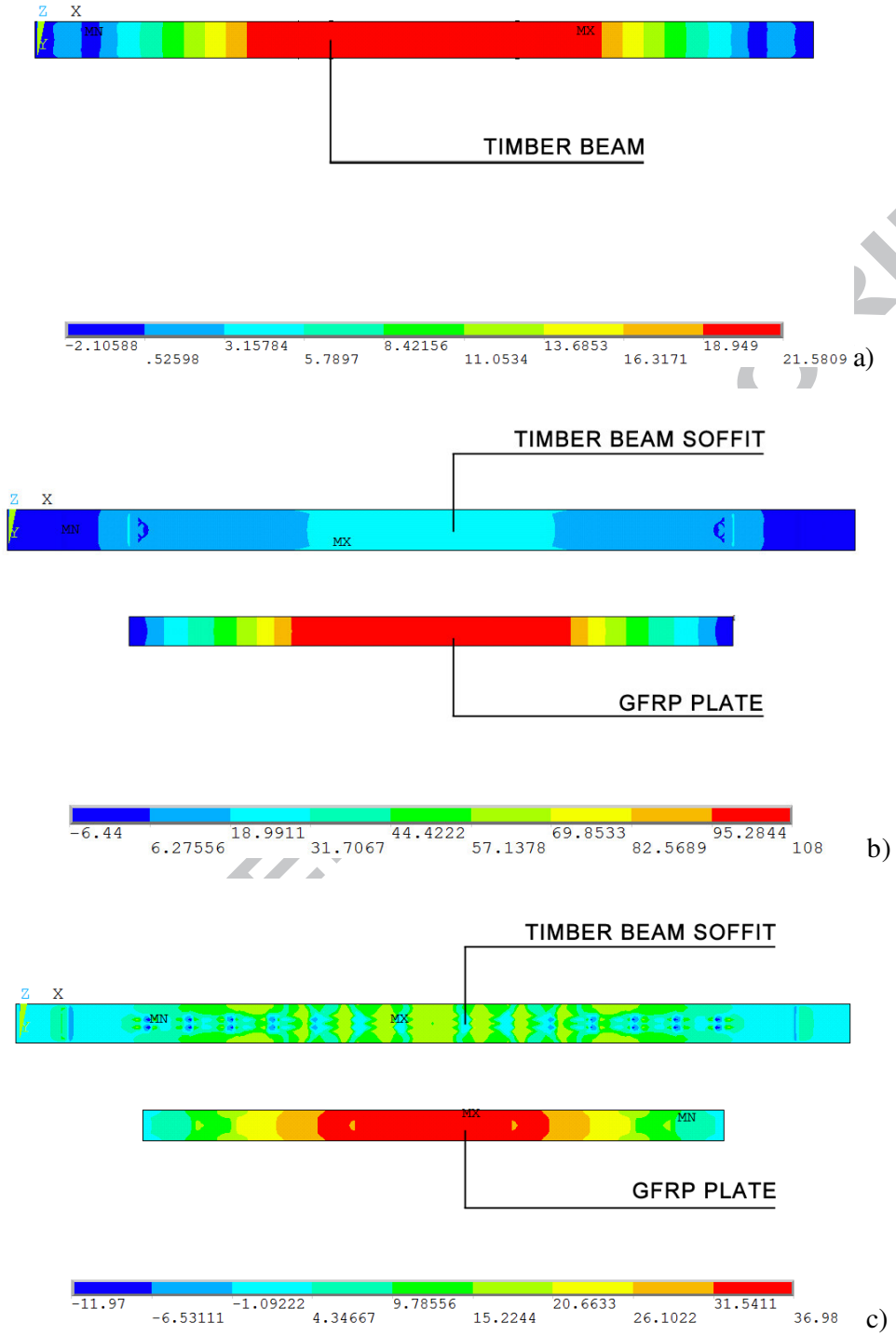

Figure 23: Contour plots of the maximum principal stress (maximum tensile stress): a) unreinforced beam; b) epoxy-bonded GFRP-reinforced beam; c) unbonded GFRP-reinforced beam (1st Arrangement) (dimensions in [MPa]).

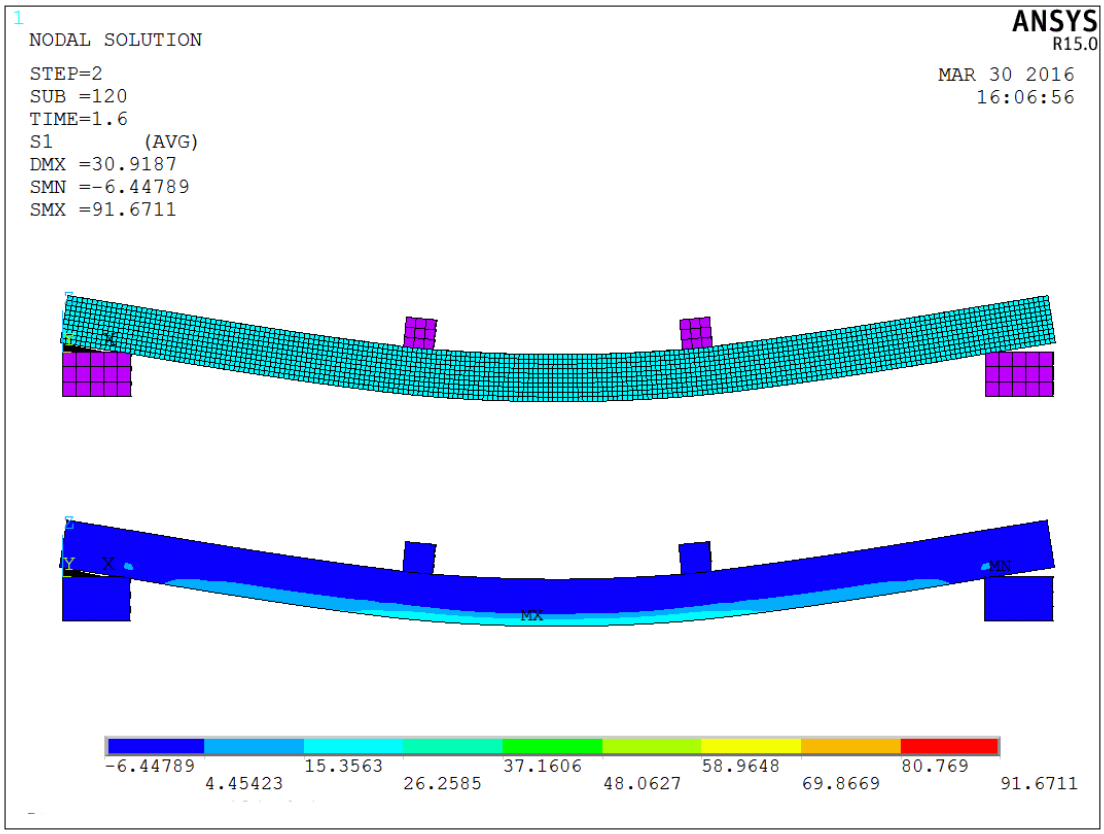

Figure 24: Deflection and failure mode of epoxy-bonded GFRP-reinforced beam (dimensions in [MPa]).